Supporting Information

Potassium hydroxide treatment of layered WSe_2 with enhanced electronic performances

Dewu Yue,[a] Cheng Tang,[b] Jiajing Wu,[a] Xiaohui Luo,[c] Hongyu Chen,[d,*] Yongteng Qian[c,*]

[a]Information Technology Research Institute, Shenzhen Institute of Information Technology, Shenzhen, 518172, P. R. China

[b]Graduate School of Mechanical Engineering, Sungkyunkwan University, Suwon 16419, Korea

[c]College of Pharmacy, Jinhua Polytechnic, Jinhua, Zhejiang Province, 321007, P. R. China

[d]Institute of Semiconductor Science and Technology, South China Normal University, Foshan, 528225, P. R. China.

Corresponding authors: E-mail: chenhy@m.scnu.edu.cn; qytwork@163.com

Experimental

Materials characterizations

The atomic force microscope (AFM,) with the no-contact mode was used to measure the thickness of the samples. synthesis process of the pristine WSe_2-based device is given in the following, at first, the WSe_2 film was exfoliated from the crystalline bulk material (HQ Graphene, the Netherlands) onto a 300 nm-thick SiO_2/Si substrate. The electrodes were then deposited through an electron beam lithography (EBL) with the Cr/Au (5 nm/70 nm). To obtain the p-type WSe_2-based FETs, the as-fabricated pristine WSe_2-based FETs was treated by an O_2 plasma (20 W, 120 s). We used XPS model is Thermo Fisher (Microlab350) with Magnesium light.

Fabrication of the pristine WSe_2-based FETs and p-type WSe_2-based FETs

The synthesis process of the pristine WSe_2-based device is given in the following, at first, the WSe_2 film was exfoliated from the crystalline bulk material (HQ Graphene, the Netherlands) onto a 300 nm-thick SiO_2/Si substrate. The electrodes were then deposited through an electron beam lithography (EBL) with the Cr/Au (5 nm/70 nm). To obtain the p-type WSe_2-based FETs, the as-fabricated pristine WSe_2-based FETs was treated by an O_2 plasma (20 W, 120 s). We used XPS model is Thermo Fisher (Microlab350) with Magnesium light.

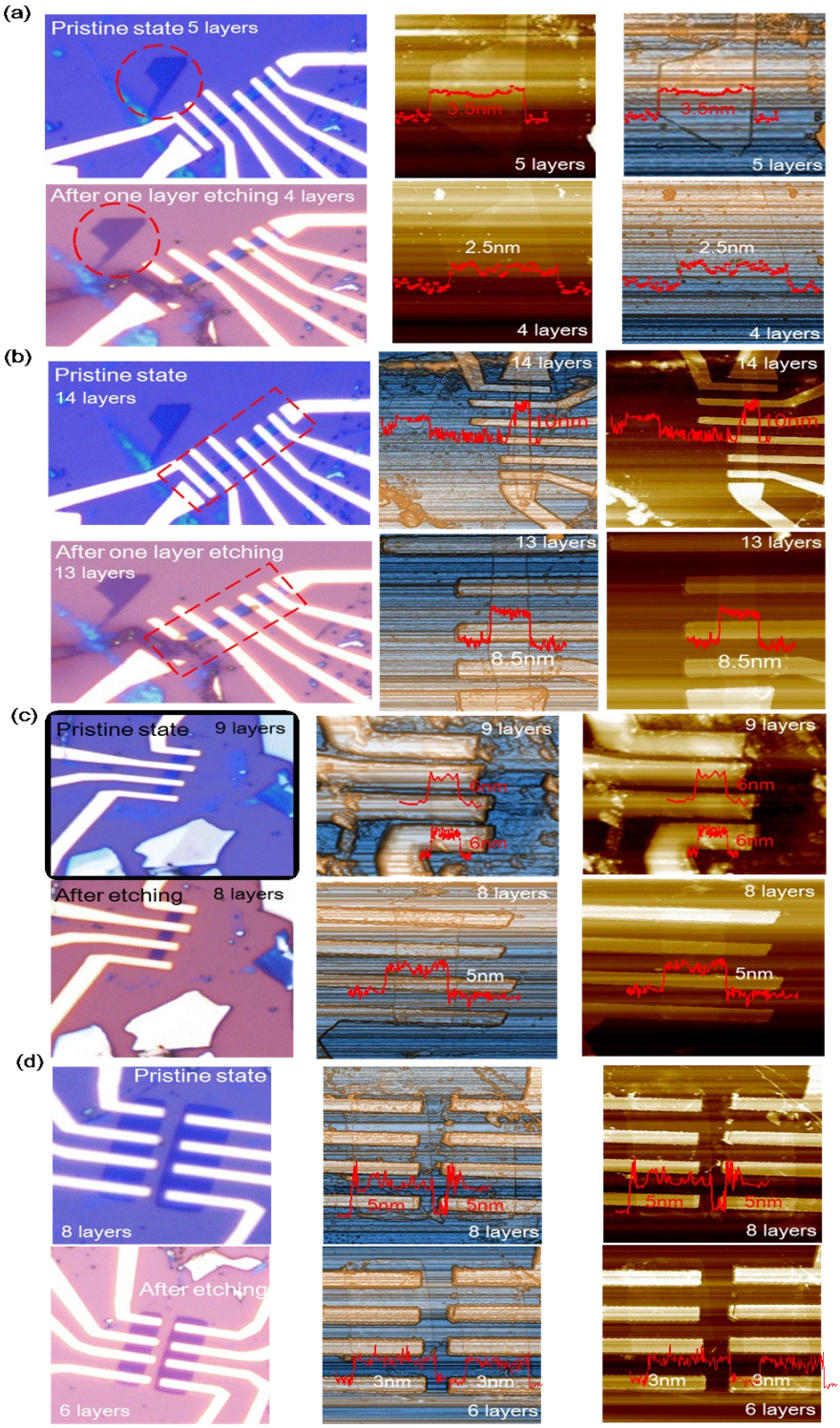

Figure S1. OM and AFM image of Sample #1(3.5nm), #2(10nm), #3(6nm) and #4(5nm). The first line of (a-d) show the OM image of the device before and after layer etching. The second and third line in (a-d) show the AFM image of the device before and after layer etching. It can be seen that around 1 nm was etching after one removal process.

Table S1. The SIMS results of the samples.

WO_x	Depth (20 points)		
	< 1 nm	1-2 nm	> 2 nm
WO^-	~ 0.56 (13 points)	~1.2 (5 points)	~2.1 (2 points)
WO_2^-	0.60 (13 points)	~1.2 (5 points)	~2.1 (1 points)
WO_3^-	0.58 (14 points)	~1.1 (6 points)	(0 points)

(a)

Raman shift 2LA(M) 1-3Layers				
Intensity	4L	3L	2L	1L
250.9625	945	1406	1245	1167
252.2221	894	1221	1149	1045
253.4814	859	1111	981	869
254.74	855	1018	870	816
255.999	863	1024	856	806
257.258	878	1011	866	811
258.5161	866	1031	860	814
259.7741	841	988	846	810
261.0318	829	928	839	807
262.2893	811	884	819	813
263.5465	790	867	802	801
264.8035	772	825	783	783
266.0602	754	809	768	770

(b)

Raman shift ($^1B_{2g}$)				
Intensity	4L	3L	2L	1L
299.892	739	756	741	743
301.142	734	755	737	743
302.391	738	755	745	746
303.64	743	764	741	746
304.888	746	750	741	737
306.137	748	758	746	740
307.385	762	768	753	743
308.633	760	772	758	742
309.88	757	766	761	743
311.128	757	757	752	743
312.375	743	751	744	742
313.621	748	756	741	742
314.868	739	747	743	742

Figure S2. Raman intensity of 2LA(M) and $^1B_{2g}$. (a) Shows the detailed data of 2LA(M) peak upshift of 2.52 cm^{-1} from multilayer to monolayer. (b) Shows the $^1B_{2g}$ upshift of 2.5 cm^{-1} with decreasing flake thickness from quadrilayer to bilayer.

Figure S2 (a) shows the detailed data of 2LA(M) peak upshift of 2.52 cm^{-1} from multilayer to monolayer, which showed in the top of Figure 3(f). From the table, it is clearly that the 2LA(M) peak upshift. Figure S2 (b) shows the detailed data of $^1B_{2g}$ upshift of 2.5 cm^{-1} with decreasing flake thickness from quadrilayer to bilayer, which showed in the down of Figure 3(f). The $^1B_{2g}$ peak upshift can be clearly seen. The $^1B_{2g}$ upshift of 2.5 cm^{-1} with decreasing flake thickness from quadrilayer to bilayer, where no $^1B_{2g}$ peak is observed from monolayer WSe_2, is consistent with that observed from exfoliated various thicknesses from monolayer to quadrilayer.

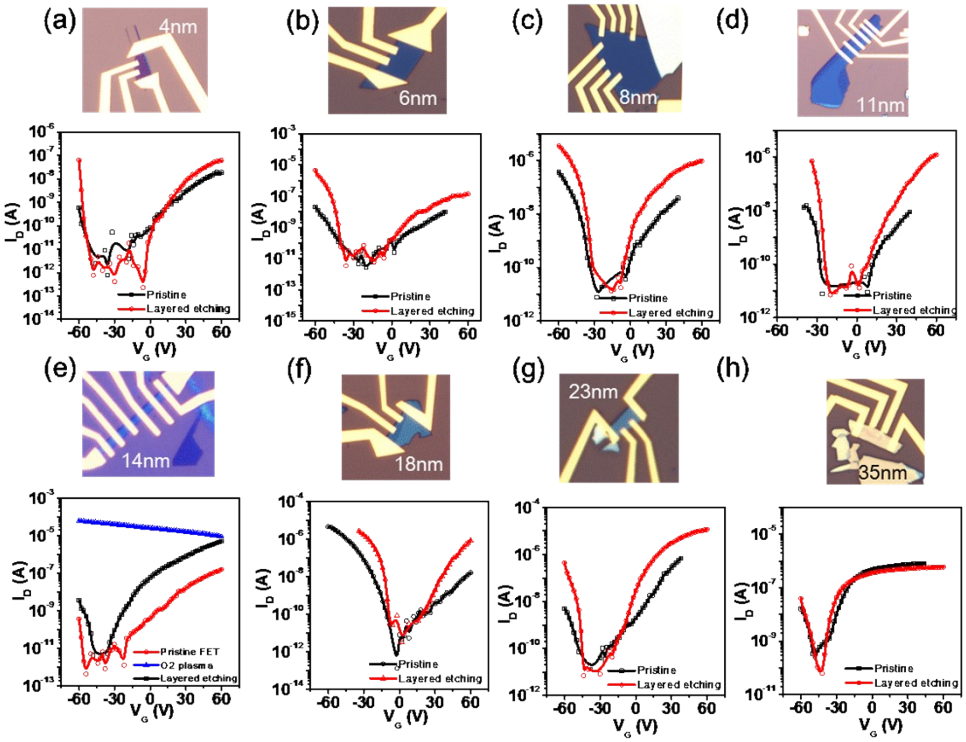

Figure S3. Enhanced ambipolar performance in different thickness devices. (a-h) Show the detailed transfer performance in 4, 6, 8, 11, 14, 18, 23 and 35 nm WSe_2 FETs to demonstrate the reliability of the etching process.

Table S2. Comparison of the mobility of the WSe_2-based devices.

Samples	Mobility ($cm^2V^{-1}s^{-1}$)	Refs.
Plasma etched WSe_2	**85**	**This work**
WSe_2	22	Nanotechnology, 2016, 27, 225501.
WSe_2	2.2	Nat. Commun., 2020, 11, 1574.
WSe_2	82	Adv. Mater., 2019, 31, 1903613.
WSe_2	36.28	Adv. Mater., 2020, 32, 1906499.
WSe_2/MoS_2 heterojunction	8.42	Nano Lett., 2020, 20, 5741.
$WSe_{2(1-x)}Te_{2x}$	46	Adv. Mater., 2017, 29, 1603991.
WSe_2/ReS_2 heterojunction	32	Nano Lett., 2020, 20, 1707.
WSe_2/h-BN heterojunction	25.6	Adv. Mater., 2016, 28, 4824.
WSe_2graphene heterostructure	84	ACS Nano, 2017, 11, 12817.